Volume 3, Issue 3, 2020 ISSN: 2664-0821
DOI: https://doi.org/10.31058/j.ap.2020.33004

Structural, Morphological Properties and band Alignment in Electrodeposited ZnO/MgO Superlattice

Egwunyenga Nkechi Josephine[1*], Ezenwaka Laz Nnadozie[2], Ezenwa Ifeyinwa Amaka[2], Okoli Nonso Livinus[3]

[1] Department of Science Laboratory Technology, Delta State polytechnic, Ogwashi-uku, Delta State, Nigeria
[2] Department of Industrial Physics, Chukwuemeka Odumegwu Ojukwu University, Anambra State, Nigeria
[3] Department of Physics, Legacy University Okija, Anambra State, Nigeria

Email Address
amakaezenwaosie@yahoo.com (Ezenwa Ifeyinwa Amaka)
*Correspondence: amakaezenwaosie@yahoo.com

Received: 2 January 2020**; Accepted:** 29 April 2020**; Published:** 13 June 2020

Abstract:
Superlattices of ZnO/MgO was successfully synthesized on Fluorine doped Tin Oxide (FTO) glass substrates by electrodeposition method. Structural analysis ZnO/MgO was achieved by way of X-ray diffractometry method. Scanning Electron Microscopy (SEM) at 10000 Magnification was used for the morphological studies. Time of deposition was varied for the optimization of film growth. Our result indicates that the film thickness increased as time of deposition increased and the highest thickness of 1.626 *um* was achieved at deposition time of 2minutes. Valence band offset (V_{BO}) of 0.1 eV and Conduction band offset (C_{BO}) of 1.3 eV were obtained for ZnO/MgO superlattice. The band alignment in our fabricated ZnO/MgO superlattice was found to be type 1.

Keywords:
Magnesium Oxide, Zinc Oxide, Electrodeposition, Band Alignment, Morphological Properties, Structural Properties

1. Introduction

Semiconductor superlattices are structures consisting of alternating layers of two different semi-conductor materials, for example ZnO/MgO, CdS/ZnS, ZnO/$Mg_{0.1}Zn_{0.9}O$ etc. According to Mazurczyk [1], semiconducting superlattice (SL) is formed when alternating layers of two semiconductors with different band gaps are deposited and thickness of these layers lies between 1 nm and 10 nm (which corresponds approximately to 1 – 100 atomic layers). Smith [2] envisaged the existence of two configurations of superlattice structure namely: compositional superlattice which consists of alternating layer of two different semiconductors and doping superlattices, which consists of alternating n – type and p – type layers of a single semiconductor. The band structure of superlattice are actually different from

those of the host material involved and can be tailored by changing parameters like thickness of the layers or barrier material. For example, the band gaps of these two semiconductors used in the formation of superlattice structure are different, and this difference is the source of real interest in heterostructure. When the superlattice structures are made of semiconductors with dissimilar bandgaps, an offset in the energy band appears at the heterojunction [3]. The key to understanding the behavior of semiconductor heterojunctions is the energy band profile which gives the plot of energy of the conduction and valence band edges versus position [4]. The depths of the conduction and valence band wells are determined by the heterostructure band offsets ΔE_c, ΔE_v which sum to the band gap difference at the interface [5]. The relative alignment of the conduction and valence band edges offers several possibilities as shown in Figure 1 [6]. This relative alignment is referred to as band edge offset.

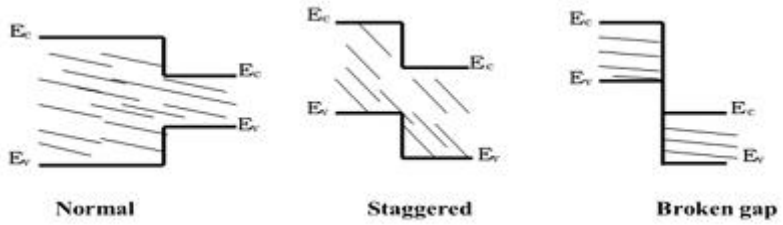

Figure 1. *The relative alignment of the conduction and valence band edges.*

Band edge offsets act as potential barriers in opposite senses on electron and holes. For normal alignment both electrons and holes are pushed by the barrier from the wide gap to the narrow gap side of the heterostructure. The superlattice miniband structures are divided into three different types, called type I, type II and type III. For type I heterostructure, the bottom of the conduction subband and the top of the valence subband are formed in the same semiconductor layer, i.e., normal alighment. In the type II, the conduction and valence subbands are either staggered in both real and reciprocal space, so that electrons and holes are confirmed in the different layers or misaligned like in the broken gap. A type III heterostructure is formed when no gap exist in one of the materials.

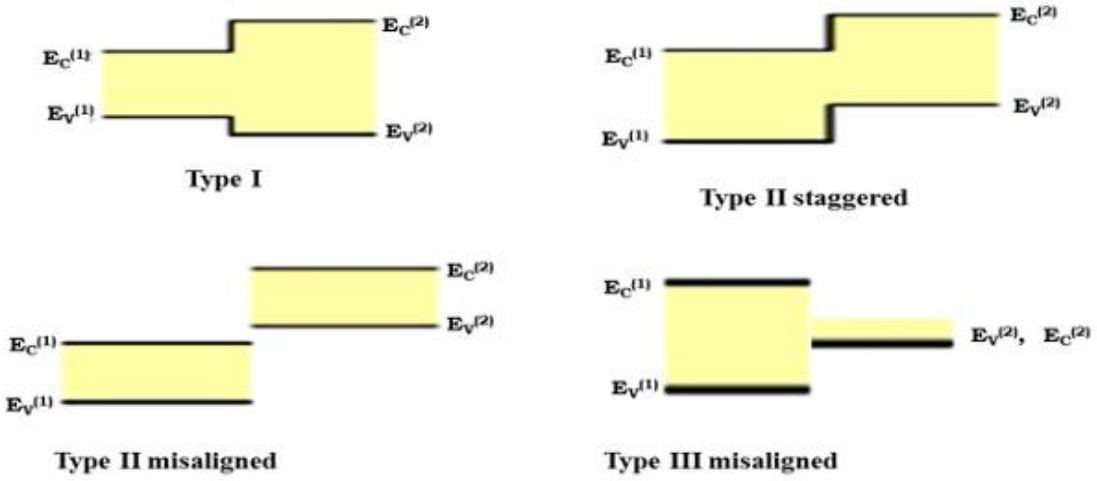

Figure 2. *Types of Superlattice miniband structures.*

Superlattices can be produced using various techniques, but the most common are molecular-beam epitaxy (MBE) and sputtering. With these methods, layers can be produced with thicknesses of only a few atomic spacings. Metal-organic chemical

vapor deposition (MO-CVD) has also contributed to the development of superconductor superlattices. Cho *et al* [7] prepared ZnO/$Mg_{0.1}Zn_{0.9}O$ nano-scale multilayer thin films by pulsed laser deposition method and obtained band gap of 3.34 eV to 3.70 eV. Tanaka *et al* [8] fabricated MgO/ZnO by molecular-beam epitaxy, and the band-gap energy was artificially tuned from 3.30 to 4.65 eV. Jiang *et al* [9] synthesized ZnO/SnO_2 using chemical vapour deposition. Haislmaier *et al* [10] synthesized series of high quality $(SrTiO_3)_n/(CaTiO_3)_n$ superlattice structures on LSAT substrates by employing hybrid molecular beam epitaxy. Talinungsang *et al* [11] prepared TiO_2/SnO_2 and SnO_2/TiO_2 by the sol-gel technique.

This paper reports the fabrication of MgO/ZnO superlattice using electrodeposition method and the analysis of optical properties and band alignment of fabricated ZnO/MgO superlattice structures. Structural properties of the deposited superlattice films were also evaluated

2. Materials and Methods

In this research work, the electrodeposition technique was employed to fabricate ZnO/MgO superlattice on fluorine doped tin oxide substrate. The procedure used in this work was similar to the one used in our previous work [12]. In this case time as a factor that effect thin film deposition was optimized. The chemical constituents for the deposited ZnO and MgO thin film are presented in Table 1.

Table 1. *Chemical Constituents for the Deposition Time Optimized ZnO / MgO Superlattice.*

Bath Name	Chemicals	Concentration (mol)	Volume (ml)	pH	Deposition Time (mins)	Current I (mA)	Voltage V (volts)	Temp (K)
1	$ZnSO_4.7H_2O$ Citric acid NaOH + $MgSO_4.7H_2O$ Citric acid NaOH	0.5 0.5 1.0 0.5 0.5 1.0	10.00 10.00 20.00 10.00 10.00 15.00	8.6	0.5	2.59	2.60	303
2	$ZnSO_4.7H_2O$ Citric acid NaOH + $MgSO_4.7H_2O$ Citric acid NaOH	0.5 0.5 1.0 0.5 0.5 1.0	10.00 10.00 20.00 10.00 10.00 15.00	8.6	1.0	2.42	2.48	303
3	$ZnSO_4.7H_2O$ Citric acid NaOH + $MgSO_4.7H_2O$ Citric acid NaOH	0.5 0.5 1.0 0.5 0.5 1.0	10.00 10.00 20.00 10.00 10.00 15.00	8.6	1.5	2.46	1.60	303
4	$ZnSO_4.7H_2O$ Citric acid NaOH + $MgSO_4.7H_2O$ Citric acid NaOH	0.5 0.5 1.0 0.5 0.5 1.0	10.00 10.00 20.00 10.00 10.00 15.00	8.6	2.0	2.29	1.61	303

5	$ZnSO_4.7H_2O$ Citric acid NaOH + $MgSO_4.7H_2O$ Citric acid NaOH	0.5 0.5 1.0 0.5 0.5 1.0	10.00 10.00 20.00 10.00 10.00 15.00	8.6	2.5	1.43	1.60	303

Film Characterization:

After the successful deposition of ZnO/MgO superlattice, the surface morphology of the films were done with the aid of Scanning Electron Microscope (SEM) at 10000 Magnification. X – ray diffraction spectrum of the film was obtained using Bruker D8 Advance X – ray diffractometer with Cu K – α wavelength of 1.54Å. The absorbance in arbitrary units was obtained with A Janway 6405 UV/visible spectrophotometer and the band gap energies of deposited superlattice structure were obtained from the absorbance data.

3. Results and Discussion

3.1. Structural Analysis of ZnO/MgO Superlattice

Figure 3 and Figure 4 show the structural patterns of fabricated ZnO thin film and ZnO/MgO superlattice. It was found that ZnO thin film is single crystalline consisting of ZnO hexagonal phase and ZnO/MgO hetero-junction thin films indicated a shift as result of the thin layer of ZnO consisting of ZnO/MgO cubic phase which is in agreement with other published work [13].

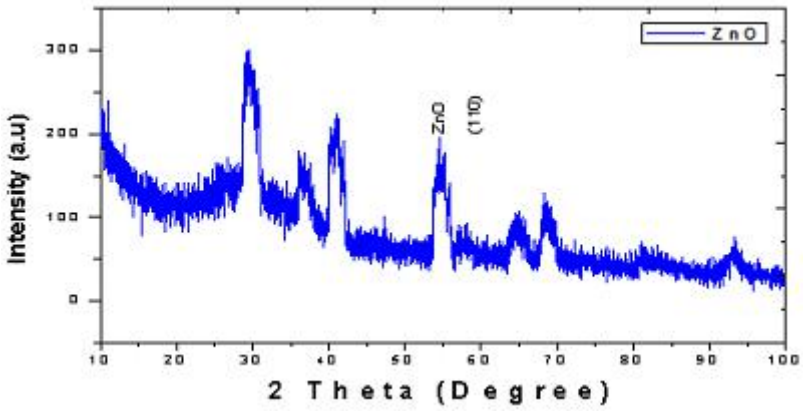

Figure 3. *The XRD Pattern of ZnO.*

The study of XRD pattern of ZnO thin film of Figure 3 show that the thin film deposited had preferential orientation along 110 with two theta value of 56.65° other peaks located are around two theta values of 32.42°, 36.25°, 41.53°, 66.26°, 68.89° and 94.68°. The 2 theta angle of 56.65° with miller indices (110) has d – spacing of 1.625Å. The FWHM value calculated was 0.43° and crystallite size of 29.14 nm was obtained. In Figure 4, the XRD pattern showed the simultaneous plot of ZnO and ZnO/MgO. This gives a clear view of the relationship in their orientations. The crystal structure that has been identified to be cubic phase was located at 2 theta values of 37.62°.

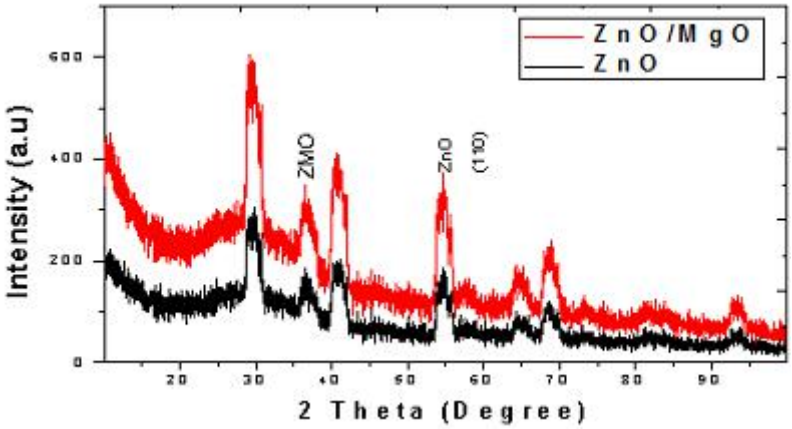

Figure 4. *The XRD Pattern of ZnO and ZnO/MgO Superlattice.*

3.2. Energy Band Gap and Band Offset of ZnO/MgO Supperlattice

The graph of absorption coefficient squared $(\alpha hv)^2$ against photon energy for MgO, ZnO, MgO/ZnO and ZnO/MgO were plotted and presented in Figure 5, Figure 6 and Figure 7 respectively. The optical band gap energy (E_g) of the films was estimated from the plot of $(\alpha hv)^2$ versus photon energy (hv) curve shown. The straight nature of the plots indicate the existence of direct transition, the direct band gap energies of the films were determined by extrapolating the straight portion of the photon energy (hv) axis at $(\alpha hv)^2 = 0$. It was found to be 4.40 eV for MgO, 3.00 eV for ZnO. From Figure 7, the optical bandgap energies for MgO/ZnO and ZnO/MgO superlattices were obtained. The values were found to be 3.00eV for MgO/ZnO and 3.10eV for ZnO/MgO superlattice. A valence band offset (V_{BO}) of 0.1eV and conduction band offset (C_{BO}) of 1.3eV was then calculated for the superlattice as shown in Figure 6. The band alignment in this system was found to be type 1.

Figure 9 shows the graph of film thickness against deposition time. The film thickness increases as time of deposition increases and the highest thickness was obtained at deposition time of 2 minutes.

Figure 10 depicts the Scanning Electron Microscopy (SEM) at 10000 Magnification of MgO/ ZnO Superlattice Deposited at 2 mins time of Deposition. The grains are thiny, extending the entire width of the film.

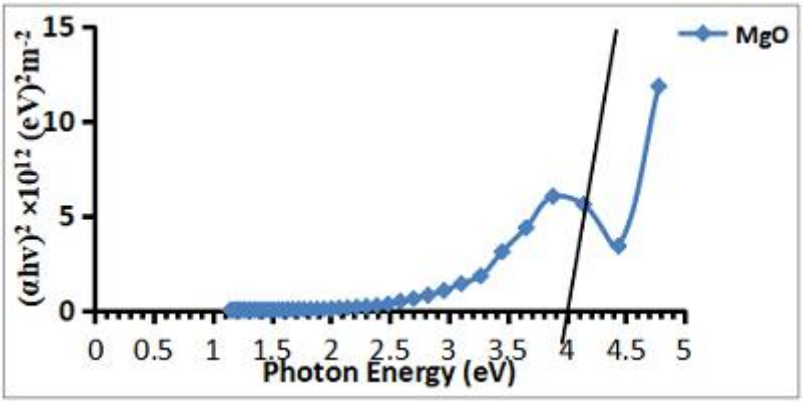

Figure 5. *Plot of absorption coefficient squared versus photon energy for MgO Thin film.*

Volume 3, Issue 3, 2020 ISSN: 2664-0821
DOI: https://doi.org/10.31058/j.ap.2020.33004

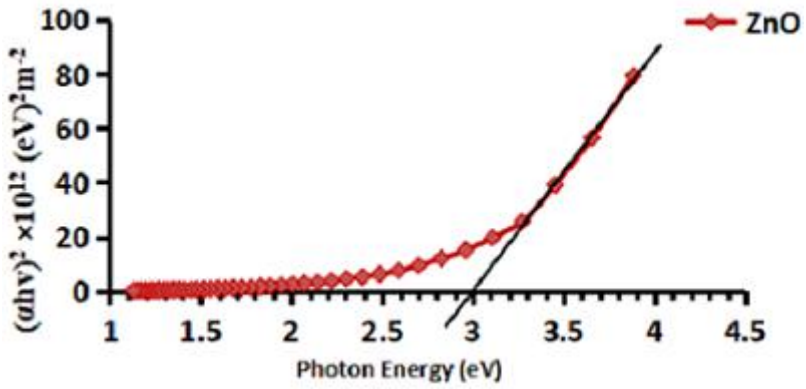

Figure 6. *Plot of absorption coefficient squared versus photon energy for ZnO Thin film.*

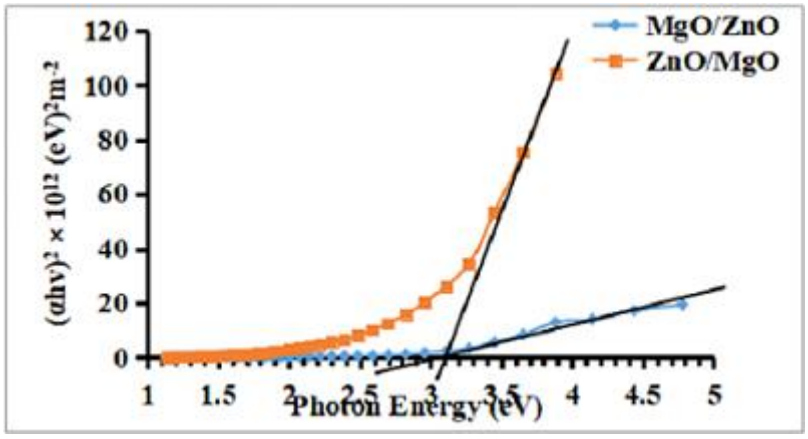

Figure 7. *Plot of absorption coefficient squared versus photon energy for MgO/ZnO and ZnO/MgO superlattices.*

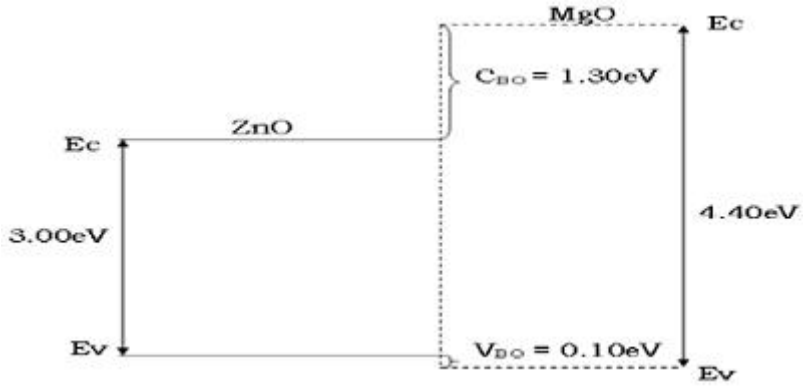

Figure 8. *Band alignment in ZnO /MgO superlattice.*

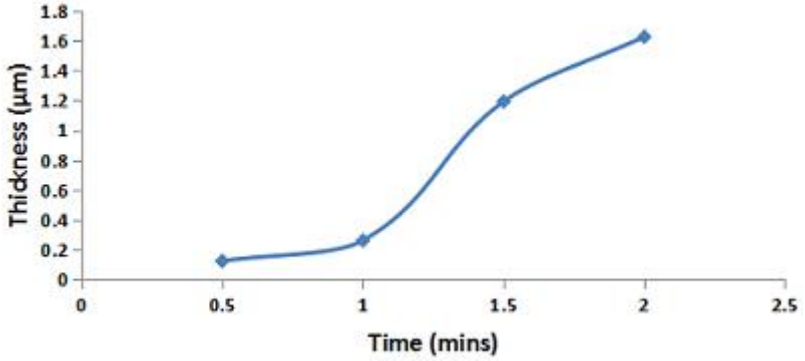

Figure 9. *Graph of Thickness (μm) against Deposition Time (mins).*

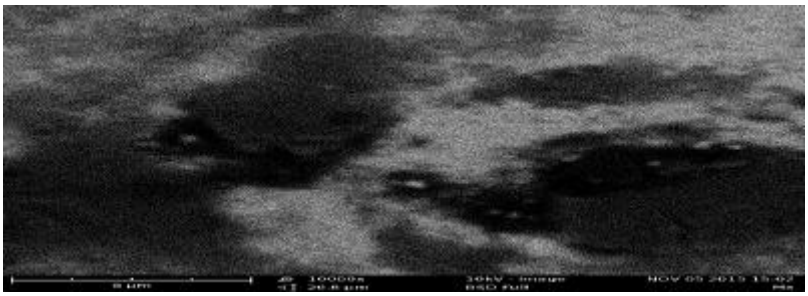

Figure 10. *Scanning Electron Microscopy (SEM) 10000 Magnification of MgO/ ZnO Superlattice Deposited at 2 mins time of Deposition.*

4. Conclusion

Superlattices of ZnO/MgO was successfully synthesized on Fluorine doped Tin Oxide (FTO) glass substrates by electrodeposition method. X-ray diffractometry method was used to obtain structural characterization. Scanning Electron Microscopy (SEM) at 10000 Magnification was used for the morphological studies. For the optimization of film growth, the time of deposition was varied. Our result indicates that the film thickness increased as time of deposition increased and the highest thickness of $1.626\,\mu m$ was found at deposition time of 2minutes. Optical bandgap energies for MgO/ZnO and ZnO/MgO superlattices were found to be 3.00eV and 3.10eV respectively. The band offset for ZnO/MgO superlattice which describes the relative alignment of the energy band at a semiconductor heterojuction of ZnO and MgO was calculated. Valence band offset V_{BO} of 0.1 eV and Conduction band offset C_{BO} of 1.3 eV were obtained for ZnO/MgO superlattice. The band alignment in this system was found to be type 1. XRD patterns of our fabricated ZnO thin film and ZnO/MgO superlattice indicated that ZnO thin film is single crystalline consisting of ZnO hexagonal phase with preferential orientation located around two theta value of 56.650 in the (110) atomic plane. ZnO/MgO superlattice indicated a shift as result of the thin layer of ZnO consisting of ZnO/MgO cubic phase. It revealed improvement in crystallinity.

Conflicts of Interest

The authors declare that there is no conflict of interest regarding the publication of this article.

Author Contributions

Conceptualization: E.N.J.; E.L.N.; E.I.A.; Methodology: E.N.J.; E.L.N.; E.I.A.; Software: E.I.A.; O.N.L.; Validation: E.L.N.; E.I.A.; Formal analysis: E.I.A.; O.N.L.; Investigation: E.N.J.; E.L.N.; E.I.A.; O.N.L.; Resources: E.N.J.; Data Curation: E.N.J.; E.I.A.; O.N.L.; Writing – original draft preparation: E.N.J.; E.I.A.; O.N.L.; Writing – review and editing: E.N.J.; E.L.N.; E.I.A.; O.N.L.; Visualization: E.L.N.; E.I.A.; O.N.L.; Supervision: E.L.N.; E.I.A.; Project administration: E.L.N.; E.I.A.; Funding acquisition: E.N.J.

Funding

This research received no specific grant from any funding agency in the public, commercial or not-for-profit sectors.

Acknowledgments

The authors would like to acknowledge the lecturers in the solid state physics, department of Industrial Physics, Chukwuemeka Odumegwu Ojukwu University Uli, Anambra State, Nigeria for their positive criticism of this work.

References

[1] Mazurczyk, R. Semiconductor Superlattices. *Chaos Solitons Fractals*, 1999, 10(12), 1971-1982, DOI: https://doi.org/10.1016/S0960-0779(98)00245-8.

[2] Smith, D.L.; Mailhiot, C. Theory of Semiconductor Superlattice Electronic Structure, Reviews of Modern Physics, 1990, 62(1), 173-234, DOI: https://doi.org/10.1103/RevModPhys.62.173.

[3] Swaminathan, V.; Jayaraman, A. Semiconductors, Raman Spectroscopy of. *Reference Module in Materials Science and Materials Engineering,* 2016, 1-8. DOI: https://doi.org/10.1016/B978-0-12-803581-8.03195-7.

[4] Frensley, W.R. Heterostructure and Quantum Well Physics. *VLSI Electronics Microstructure Science*, 1994, 24, 1-24, DOI: https://doi.org/10.1016/B978-0-12-234124-3.50006-9.

[5] Chuang, S.L. Physics of photonic devices, 2nd ed. Hoboken NJ, Wiley, 2009.

[6] Kittel, C. Introduction to Solid State Physics, 7th edition, John Wiley and Sons Inc., New York, 1996, 211, 228.

[7] Cho, J.Y.; Shin, S.W.; Kwon, Y.B.; Hyun-Ki Lee, Kyu UngSim, Hong SeungKim, Jong-HaMoon and Jin HyeokKim. The effect of $Mg_{0.1}Zn_{0.9}O$ layer thickness on optical band gap of $ZnO/Mg_{0.1}Zn_{0.9}O$ nano-scale multilayer thin films prepared by pulsed laser deposition method. *Materials Science,* 2011, 519(13), 4282-4285, DOI: https://doi.org/10.1016/j.tsf.2011.02.010.

[8] Tanaka, H.; Fujita, S.; Fujita, S. Fabrication of wide-band-gap $Mg_xZn_{1-x}O$ quasi-ternary alloys by molecular-beam epitaxy. *Appl. Phys. Lett.* 2005, 86, 192911. DOI: https://doi.org/10.1063/1.1923762

[9] Jiang, S.; Ge, B.; Xu, B.; wang Q.; Cao, B. In Situ Growth of $ZnO/SnO_2(ZnO:Sn)m$ Binary/Superlattice Heterojunction Nanowire Arrays. *Cryst. Eng. Comm.,* 2017, 18(1), 1-21, DOI: https://doi.org/10.1039/C8CE90194E.

[10] Haislmaier, R.C.; Lapano, J.; Yuan, Y.; Stone, G.; Dong, Y.; Zhou, H.; Alem, N.; Engel-Herbert, R. Overlapping growth windows to build complex oxide superlattices. *APL Materials,* 2018, 6(111104), 1-8, DOI: https://doi.org/10.1063/1.5061778.

[11] Talinungsang, P.N.; Purkayastha, D.D.; Krishna, M.G. TiO_2/SnO_2 and SnO_2/TiO_2 heterostructures as photocatalysts for degradation of stearic acid and methylene blue under UV irradiation. *Superlattices and Microstructures,* 2019, 129, 105-114, DOI: https://doi.org/10.1016/j.spmi.2019.03.004.

[12] Egwunyenga, N.J.; Ezenwaka, L.N.; Ezenwa, I.A.; Okoli, N.L. Effect of annealing temperature on the optical properties of electrodeposited ZnO/MgO superlattice. *Mater. Res. Express,* 2019, 6(10), 105921, DOI: https://doi.org/10.1088/2053-1591/ab42ab.

[13] Bhattacharya, R.N.; Ramanathan, K., Cu(In,Ga)Se_2 Thin Film Solar Cells with Buffer Layer Alternative to CdS. *Solar Energy,* 2004, 77(6), 679-683, DOI: https://doi.org/10.1016/j.solener.2004.05.009.